

Angular and momentum asymmetry in particle production at high energies.

Andrei Leonidov^{(1,2)1} and Dmitry Ostrovsky⁽²⁾²

(1) *School for Physics and Astronomy, University of Minnesota, Minneapolis MN 5455, USA*

(2) *P.N. Lebedev Physical Institute, 117924 Leninsky pr. 53, Moscow, Russia*

Abstract

Angular asymmetry and momentum disbalance for a pair of particles produced at high energy in central rapidity region are studied. The asymmetry is substantial for small momenta of produced particles but diminishes when they rise.

¹e-mail: leonidov@td.lpi.ac.ru

²e-mail: ostrov@td.lpi.ac.ru

1 Introduction

The QCD description structure of the final state in high energy processes is one of the most important subjects in strong interaction physics. Of special interest is the analysis of the final state formation at high energies, where one should resum the contributions logarithmic in energy (Bjorken x). This problem has drawn a considerable interest and was studied in a number of recent publications [1], [2].

In the approach traditionally applied for describing the final state in the high energy hadron collisions, that of collinear factorization, the final state is produced with the zero total transverse momentum. In particular for two-particle final state this means that these particles leave the collision point in the opposite directions and having equal absolute values of their transverse momenta. We will refer to such a configuration as symmetric and will consider any deviation from it as asymmetry. The value of the asymmetry can be used as the measure of the departure from the collinear factorization showing limit of its applicability. To quantify the effects related to the nonvanishing total transverse momentum of the final state one has to use an approach in which the transverse momenta of incoming partons are not neglected. Let us note, that in a number of recent experiments on diphoton [3], π^0 and direct photon [4] production a substantial discrepancy between the data and predictions of collinearly factorized NLO QCD was observed. Taking into account the intrinsic transverse momenta of order of 1 – 2 GeV substantially improves this situation. The results of [4] also show sufficiently broad angular distribution in π^0 production.

The paper is organized as follows. In the next section the high energy factorization will be reviewed and compared with the collinear factorization one. In section 3 numerical results for the shape of the final state containing two particles in the central rapidity region are presented. The derivation of the expressions for the cross sections used in our calculations can be found in the Appendices. In section 4 we summarize the results and present our conclusions.

2 Collinear and high energy factorization

Collinear factorization [5] is a method of describing the strong interaction processes by factorizing the contribution to physical cross sections into the product of partons distributions $f_a(x, k^2)$ parametrizing both the nonperturbative information about the hadron and perturbative evolution starting from some specific initial condition and perturbative cross sections corresponding to the scattering of the parton fluxes. In this approach the prehistory of colliding partons is entirely determined by structure functions while partons themselves are supposed to be on-shell particles. The cross section for two-particle (jet) production to the lowest perturbative (Born) order is

$$\frac{d\sigma}{dk^2 dy_1 dy_2} = x_1 f_a(x_1, k^2) \frac{d\hat{\sigma}_{ab}}{dt} x_2 f_b(x_2, k^2), \quad (1)$$

where the sum over parton types a, b is assumed and $x_{1,2} = k_{\perp}(e^{\pm y_1} + e^{\pm y_2})/\sqrt{S}$, where \sqrt{S} is an invariant collision energy.

In this approach it is assumed that

$$\Lambda_{QCD} \ll k_{\perp} \sim x\sqrt{S} \sim \sqrt{S}. \quad (2)$$

indicating that one can apply perturbative QCD and that there is only one big logarithm to take into account, that is $\ln(k^2/\Lambda_{QCD}^2)$. Resummation of the powers of this logarithm (i.e. $\sim \alpha_s^n \ln^n(k^2/\Lambda_{QCD}^2)$) leads to structure functions depending on k^2 and is performed by DGLAP evolution equation [6].

The situation changes at large S when one reaches the kinematic region

$$\Lambda_{QCD} \ll k_{\perp} \sim x\sqrt{S} \ll \sqrt{S} \quad (3)$$

Under these conditions another big logarithm $\ln(1/x)$ exists. Resummation of powers of this logarithm can become more important than the one of $\ln(k^2/\Lambda_{QCD}^2)$. The resummation of the leading energy logarithms for the structure function is described by BFKL equation [7].

In this kinematical region the transverse momenta of the incoming parton fluxes can no longer be neglected. To take them into account a new approach called " k_{\perp} factorization" was proposed in [8]. Extensive description of the method and various applications can be found in [9]. Let us note that this method was *de facto* used earlier in [10].

The method of k_{\perp} factorization is based on considering "partons" with nonzero transverse momentum and being, in contrast to the collinear factorization case, off-mass shell particles. Calculation of physical cross-sections requires a generalization of the conventional picture of parton flux as described by usual parton structure functions. To this aim an unintegrated gluon distribution $\phi(x, q_{\perp}, k)$ is introduced:

$$xg(x, k^2) = \int \frac{dq_{\perp}^2}{q_{\perp}^2} \phi(x, q_{\perp}, k), \quad (4)$$

where ϕ/q^2 is proportional to the probability of finding the incident parton with longitudinal momentum component xp_a (p_a is a momentum of initial particle) and transverse momentum q_{\perp} . It is important to stress that unintegrated structure function depends not only upon the momentum of particle to which it corresponds, q , but also on the global off-mass-shellness of the process, k^2 . This is in fact a general property of distributions in quantum theory – the probability of a particular event depends not only of its parameters, but also on the global characteristics of the event ensemble.

The particular interrelation between the unintegrated and integrated structure functions depends on the evolution equation that the integrated distribution solves. For the DGLAP evolution [6] the unintegrated structure function can be expressed through the integrated one as follows: [23]

$$\phi(x, q_{\perp}, k) = \left(\frac{\alpha_s}{2\pi} \int_x^{1-q_{\perp}/k} \frac{dz}{z} P_{gg}(z) xg\left(\frac{x}{z}, q_{\perp}^2\right) \right) T_g(q_{\perp}, k) \quad (5)$$

where T_g is the Sudakov form factor [24] for gluon

$$T_g(q_\perp, k) = \exp \left(- \int_{q_\perp^2}^{k^2} \frac{\alpha_s(p_\perp)}{2\pi} \frac{dp_\perp^2}{p_\perp^2} \sum_{i=g,q,\bar{q}} \int_0^{1-q_\perp/k} P_{ig}(z) dz \right) \quad (6)$$

(for P_{gg} in the last expression one should substitute $P_{gg}(z) \rightarrow zP_{gg}(z)$ in account of gluons identity). In a double logarithmic approximation Eqs. (5-6) coincide with the DDT formula [25].

For BFKL evolution [7] the correspondence between integrated and unintegrated structure functions takes a simpler form

$$\phi(x, q_\perp) \equiv \phi(x, q_\perp, q_\perp) = \frac{\partial x g(x, q_\perp^2)}{\partial \ln q_\perp^2}. \quad (7)$$

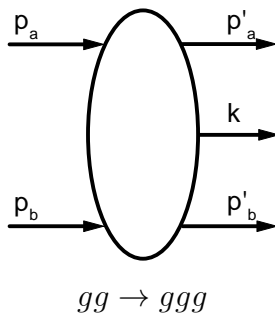
This results from the absence of strong q_\perp ordering in BFKL ladder.

From the practical point of view, Eqs. (5-6) differ substantially from Eq. (7) only for $q_\perp \ll k$ implying the presence of a big logarithmic contribution $\propto \ln k^2/q_\perp^2$. Therefore we can in fact use Eqs. (5-6) for both types of QCD evolution.

The calculation of a cross section with virtual colliding particles presents a highly non-trivial problem. The first difficulty lies in the correct summation over polarization states of the incident off-shell "partons". Another problem is the presence of bremsstrahlung from initial and final states of colliding particles. The derivation of the relevant cross sections is outlined in Appendix A.

More specifically, the transverse (high energy) factorization is based on considering the $2 \rightarrow n + 2$ process cross section with a large rapidity gaps between the two final particles providing a full rapidity interval for the process under consideration which are almost collinear to the incident ones and n particles emitted into the central rapidity region (so called quasi-multy-Regge kinematics or QMRK [11, 12]). Note that only the amplitude with on-shell and physically polarized in- and outgoing particles has precise gauge invariant meaning and only such expressions can be used in calculating the cross section. Large rapidity gaps provide a separation between quantities related to the incident particles and those describing the hard cross section of parton production in the central region.

Let us for example consider the process $gg \rightarrow ggg$ in the limit of high energy



$$\frac{d\sigma_{gg \rightarrow ggg}}{d^2k_\perp dy} = \frac{4N_c^3 \alpha_s^3}{\pi^2(N_c^2 - 1)} \int \frac{d^2q_{1\perp}}{q_{1\perp}^2} \frac{\delta^{(2)}(q_{1\perp} + q_{2\perp} - k_\perp)}{k_\perp^2} \frac{d^2q_{2\perp}}{q_{2\perp}^2} \quad (8)$$

with $q_{1,2} = p_{a,b} - p'_{a,b}$.

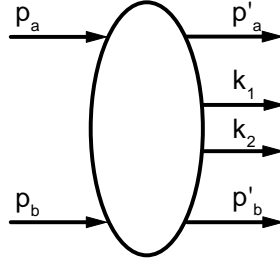
This equation demonstrates the above mentioned factorization of the cross section. The first, second and third factors under the integral correspond to $p_a \rightarrow p'_a$, q_1 splitting, $q_1, q_2 \rightarrow k$ "scattering" and $p_b \rightarrow p'_b$, q_2 splitting respectively.

The factors related to the splitting of the incident particles should further be converted to structure functions. One can do it in two steps. The first step, transformation to the form factors, is quite straightforward [13]. In the second step we have to account for corrections due to radiation along the directions of incident particles and replace form factors by unintegrated structure functions $\varphi(x, q_\perp, k)$ with x determined by kinematics.

The cross sections for producing $n = 0, 1, 2$ particles in the central region read

$$\sigma_0 = \frac{(2\pi)^2}{N_c^2 - 1} \int d^2q_\perp \frac{\varphi(x, q_\perp)}{q_\perp^2} \frac{\varphi(x, q_\perp)}{q_\perp^2} \quad x = q_\perp^2/S; \quad (9)$$

$$\begin{aligned} \frac{d\sigma_1}{d^2k_\perp dy} &= \int d^2q_{1\perp} d^2q_{2\perp} \frac{\varphi(x_{1,0}, q_{1\perp}, k_\perp)}{q_{1\perp}^2} \frac{d\hat{\sigma}_1}{dk_\perp^2} \frac{\varphi(x_{2,0}, q_{2\perp}, k_\perp)}{q_{2\perp}^2}, \\ \frac{d\hat{\sigma}_1}{dk_\perp^2} &= \frac{4N_c \alpha_s}{N_c^2 - 1} \frac{\delta^{(2)}(q_{1\perp} + q_{2\perp} - k_\perp)}{k_\perp^2}, \\ x_{1,0} &= k_\perp e^y / \sqrt{S}, \quad x_{2,0} = k_\perp e^{-y} / \sqrt{S}; \end{aligned} \quad (10)$$



$gg \rightarrow gggg$

$$\begin{aligned} \frac{d\sigma_2}{d^2k_{1\perp} d^2k_{2\perp} dy_1 dy_2} &= \frac{1}{\pi^2} \int d^2q_{1\perp} d^2q_{2\perp} \frac{\varphi(x_1, q_{1\perp}, k_\perp)}{q_{1\perp}^2} \frac{d\hat{\sigma}_2}{d^2k_{1\perp} d^2k_{2\perp}} \frac{\varphi(x_2, q_{2\perp}, k_\perp)}{q_{2\perp}^2}, \\ k_\perp &= k_{1\perp} + k_{2\perp} \\ \frac{d\hat{\sigma}_2}{d^2k_{1\perp} d^2k_{2\perp}} &= \frac{2N_c^2 \alpha_s^2}{N_c^2 - 1} \frac{\delta^{(2)}(q_{1\perp} + q_{2\perp} - k_{1\perp} - k_{2\perp})}{q_{1\perp}^2 q_{2\perp}^2} \mathcal{A}, \\ x_1 &= (k_{1\perp} e^{y_1} + k_{2\perp} e^{y_2}) / \sqrt{S}, \quad x_2 = (k_{1\perp} e^{-y_1} + k_{2\perp} e^{-y_2}) / \sqrt{S}. \end{aligned} \quad (11)$$

The expression for $n = 0$ corresponds to the total cross section in the two gluon exchange (Low-Nussinov) approximation. Let us note that the kinematics of Eq. (3) is not quite the one in Eq. (9). Having no k_{\perp} in this process we have to restrict directly q_{\perp} . In Eq. (9) $q_{\perp} = \sqrt{xS}$ while it is $q_{\perp} \sim x\sqrt{S}$ that is given by (3).

The case of one gluon production in the central region ($n = 1$) was studied in a number of publications, e.g. [13], [14].

A part of the analytical expression for \mathcal{A} (for $gg \rightarrow gg$ subprocess) has recently been published in [12, 15]. A similar quantity for $gg \rightarrow q\bar{q}$ subprocess can be found in [12, 16]. The derivation of the explicit expressions is outlined in the Appendices A and B. Let us note that the formula for $gg \rightarrow q\bar{q}$ cross section from [16] coincides with the analogous formula in [9] (in the limit of massless quarks) obtained by direct application of k_{\perp} factorization.

For practical applications of the equations Eq. (9-11) we should understand the overall normalization of the off-shell cross sections to the usual on-shell one arising in collinear factorized formalism. The normalization can be deduced from considering the small q_{\perp} limit in Eq. (11). Physically, we have to return to Eq. (2) and choose the structure functions being extremely narrow functions of q_{\perp} and integrate out $d^2q_{1\perp}$ and $d^2q_{2\perp}$. There is no contradiction with Eq. (2) because $q_{\perp} \ll k_{\perp}$. Certainly, we must put $q_{1\perp}, q_{2\perp} = 0$ in $\hat{\sigma}_2$ Eqs. (11, B.2, B.3). As it is follows from Appendix A, \mathcal{A} is proportional to $q_{1\perp}^2 q_{2\perp}^2$ so this limit for $\hat{\sigma}_2$ is correct. After this substitution and integration over $k_{2\perp}$ Eq. (1) appears with the structure functions from Eq. (4) and with the correct $d\hat{\sigma}/dt$. Consequently, normalization of Eqs. (9-11) is also correct. Let us emphasize that the integration over $d^2q_{1\perp}$ and $d^2q_{2\perp}$ includes averaging over angular orientations of $q_{1\perp}$ and $q_{2\perp}$ in the transverse plane when arriving to the final expression for $\hat{\sigma}_2$. This averaging is similar to the averaging over initial gluon polarizations in getting the usual expression for the cross section of the $2 \rightarrow 2$ elastic scattering.

3 Angular and momentum asymmetry of parton production at central rapidity

The most interesting predictions of the high energy factorization are of course those going beyond the collinear factorization framework. The simplest situation corresponds to the production of a single particle in central rapidity region described in the first order in α_s Eq. (10). This process was first studied in [13] and later in many publications, see e.g. [14].

In this paper we concentrate our attention on another important feature of the high energy factorization. From Eq. (11) it is obvious that, in contrast with the collinear factorization case, the two partons produced in the central rapidity region are not necessarily going into opposite directions (back-to-back). Another important issue is that the absolute values of the momenta of outgoing partons are not necessarily equal. We will refer to these properties as angular and momentum asymmetries respectively.

The same characteristics of the two-particle production were studied in [17] in the case,

where the produced particles are separated by the large rapidity gap. The angular and momentum asymmetries considered in [17] are due to the presence of BFKL ladder filling the gap between the produced particles. Let us stress, that in this paper we study the two-particle decorrelation in a relatively small central rapidity interval. The rapidity gap, discussed in [17], is thus absent and decorrelation effects are exclusively due to off-shellness of the two generalized parton fluxes merging in a particle-producing vertex.

Our approach is similar to that in [20], where a multy-regge limit for \mathcal{A} was considered, $\mathcal{A} = q_{1\perp}^2 q_{2\perp}^2 / k_{1\perp}^2 k_{2\perp}^2$ (cf. Appendix B). In this form \mathcal{A} has no *intrinsic* angular and momentum correlations (see below). Moreover, the contributions from \mathcal{A} and the structure functions to σ_2 (see Eq. (11)) factorize and σ_2 depends on structure functions only via gluon-gluon luminosity function [23]. The latter contains practically all information about particle correlations.

A large number of independent variables in Eq. (11) makes it difficult to visualize the pattern of particles emission. Therefore we will use the less differential ones, in particular the angular asymmetry

$$\left. \frac{d\sigma_2}{d\Delta\phi dy_1 dy_2} \right|_{k_0} = \pi \int \frac{d\sigma_2}{d^2k_{1\perp} d^2k_{2\perp} dy_1 dy_2} dk_{1\perp}^2 dk_{2\perp}^2, \quad (12)$$

where $\Delta\phi \in [0, \pi]$ is the angle between particles. Integration over $k_{1\perp}$ and $k_{2\perp}$ requires introducing the infrared cutoff limit k_0 . The shape of asymmetry is sensitive to the chosen value of k_0 . In the normalization of Eq. (12) and in forthcoming Eq. (15) we took into account particles identity (even for quarks we do not distinguish between q and \bar{q}).

In order to perform actual calculations one needs to choose the unintegrated structure functions entering Eqs. (9-11). In principle they should be chosen as solutions to the NLO BFKL equation [18] or its nonlinear generalizations [19] (also taking to account form factors arising from non-compensating real and virtual corrections). Leaving this analysis for the future, let us note, that the minimal requirement surely has to be that whatever expression for the unintegrated distribution is used, it should not contradict the information from deep inelastic scattering, i.e. that on integrated structure function. This fixes the distribution in the limit $q_{\perp} = k_{\perp}$, where $\phi(x, q_{\perp}, q_{\perp}) = \phi(x, q_{\perp})$ (cf. Eq. (7)). In our numerical calculations we have used the unintegrated gluon structure functions corresponding to integrated CTEQ5M [21] and AKMS [22] fitted as in [14]. For $q_{\perp} < k_{\perp}$ the unintegrated structure function $\phi(x, q_{\perp}, k_{\perp})$ was determined according to Eqs. (5), (6). In the final distributions we sum over gluon and quark ($n_f = 5$) pair contributions (in fact, the contribution due to quark pair production is less than 3% of that due to gluons).

In Fig. 1 we show differential cross section (12) with $y_{1,2} = y_0 \mp \Delta y/2$ for $y_0 = 0$ and $\Delta y \in [0, 2]$ and with $k_0 = 2\text{GeV}$. From now on figures marked by **a**, **b** are calculated with CTEQ structure functions, marked by **c**, **d** are calculated with AKMS structure functions; figures with labels **a**, **c** correspond to $\sqrt{S} = 1.8\text{TeV}$, while those with labels **b**, **d** correspond to $\sqrt{S} = 14\text{TeV}$.

The most striking feature of this cross section that differs it from the collinear factorized one is the appearance of the collinear singularity at $\Delta y, \Delta\phi \rightarrow 0$. This singularity is just a well-known s-channel one and is in turn a reflection of the presence of one particle

production process Eq. (10). Moreover, the behavior of the two-particle production (11) near the above-described collinear singularity can be presented in the following decomposed form. Introducing $r^2 = \Delta y^2 + \Delta\phi^2$, $k_\perp = k_{1\perp} + k_{2\perp}$, $z = k_1/k$ (since k_1 and k_2 are collinear this definition is unambiguous) and taking the limit $r \rightarrow 0$, we get

$$\frac{d\sigma_2}{d^2k_\perp dy_0 dr dz} = \frac{d\sigma_1}{d^2k_\perp dy_0} \frac{1}{r} \frac{\alpha_s}{\pi} (P_{gg}(z) + 2n_f P_{qg}(z)),$$

with one particle production cross section as defined in (10). P_{gg} and P_{qg} are the standard Altarelli-Parisi kernels [6] (the factor of 2 before P_{qg} is due to identical treatment of quarks and antiquarks in our approach). From Fig. 1 we can conclude, that the dependence of the asymmetry on the structure function is quite pronounced, see corresponding upper and lower panels. For AKMS structure functions the angular distribution is noticeably wider then for CTEQ ones. This is the reflection of the fact that AKMS structure function is broader then CTEQ one if compared at some fixed value of x . The dependence of angular asymmetry on c.m.s. collision energy is, as seen from Fig. 1, relatively weak.

In Fig. 2 we take a closer look at the angular asymmetry by plotting the two-dimensional cross sections of the plots in Fig. 1 for fixed values of Δy , i.e. study the dependence of (12) on ϕ for different values of Δy where

$$\rho(\Delta\phi) \sim \frac{d\sigma_2}{d\Delta\phi dy_1 dy_2}$$

is normalized according to

$$\int \frac{d\Delta\phi}{\pi} \rho(\Delta\phi) = 1 \quad (13)$$

for each value of Δy . A substantial deviation of ρ from the back-to-back shape, for which $\rho \sim \delta(\Delta\phi - \pi)$, is obvious. From Fig. 2 we see that the asymmetry grows with increasing collision energy, although the growth is not pronounced. Using different structure functions affects the shape of the asymmetry distribution much stronger than changing the collision energy.

When the cutoff k_0 increases, the kinematic interval Eq. (3) narrows and the two outgoing particles tend to appear back-to-back. This dependence is clear from Fig. 3 where $\rho(\Delta\phi)$ is shown for $\Delta y = 1$ and several values of k_0 .

We see that when $k_\perp \gg q_{char}$, where q_{char} is a characteristic transverse momentum carried by the parton fluxes, jets are predominantly produced at small $\delta\phi = \pi - \Delta\phi$. This regime was studied in DLA in [25]. According to [25] the (normalized) azimuthal asymmetry in $\delta\phi \ll 1$ domain is given by

$$\rho(\delta\phi) \sim \frac{1}{\delta\phi} \frac{d}{d\delta\phi} T_g^2(\delta\phi) \quad (14)$$

with $T_g(\delta\phi) = T_g(\delta\phi, k_0, k_0)$ (cf. Eq. (6)). From Eqs. (6) and (14) it is obvious that the rapid growth of ρ with diminishing $\delta\phi$ stops at $\delta\phi^* \approx \exp(-\pi/6\alpha_s)$. Numerically, for $\alpha_s = 0.18$ (this value of strong coupling was used in CTEQ5M calculation for $k = 20\text{GeV}$),

$\delta\phi^* \approx 5 \cdot 10^{-2}$, in agreement with Fig. 3. Note that contrary to DLA in our approach the value of ρ for $\delta\phi < \delta\phi^*$ is not decreasing. The reason is that in our case there is no scaling leading to Eq. (14). In Fig. 3 the effect of saturation is manifest not for $\rho(\delta\phi)$ itself, but for its derivative, i.e. for the corresponding characteristic angle.

Turning now to the analysis of the momentum asymmetry let us consider the cross section integrated over the angular variables,

$$\frac{d\sigma_2}{dk_{1\perp}dk_{2\perp}dy_1dy_2} = 2k_1k_2 \int \frac{d\sigma_2}{d^2k_{1\perp}d^2k_{2\perp}dy_1dy_2} d\phi_1d\phi_2. \quad (15)$$

For $y_{1,2} = \pm 0.5$ and $k_{1,2\perp} \in [2, 20]$ GeV this cross section is plotted in Fig. 4. From this figure we see that, in a characteristic event, $k_{1\perp}$ and $k_{2\perp}$ are not equal. The dominant trend can be described as a decrease of the cross section with growing k_{\perp} . However, for the values of $k_{1,2\perp}$ of order of, or higher than 10 GeV, the correlation pattern is no longer powerlike. Finally, let us note that the momentum asymmetry shows a significant dependence on the choice of the structure function and on c.m.s. collision energy.

4 Conclusions

Angular and momentum asymmetry is a characteristic feature of particle production in semihard kinematic region. When the momenta of produced particles are of the same order as the characteristic transverse momenta carried by the generalized off-shell partonic fluxes described by the unintegrated structure function, the angular distribution of particles shows significant deviations from the conventional back-to-back picture. The asymmetry dies away when the transverse momenta of produced particles are, correspondingly, much larger than the intrinsic ones. The momentum asymmetry pattern is somewhat different due to rapid growth of the cross section with decreasing momenta. Nevertheless some reflection of momentum balance in the case of relatively high momenta is shown through local cross section deviation from power-like regime around the point where the transverse momenta of produced particles are equal.

Acknowledgements

We are grateful to L. McLerran, Yu. Dokshitzer and Yu. Kovchegov for useful and stimulating discussions. A.L. is grateful to L. McLerran for kind hospitality at the University of Minnesota.

We are grateful to O.V. Ivanov for pointing us out a powerful method of multidimensional integration [26].

The work of D.O. was partially supported by the INTAS within the research program of ICFPM, grant 96-0457.

Appendix A Particle production in QMRK

As mentioned before the QMRK regime is that in which the incident particles scatter at parametrically small angle producing particle(s) in the central rapidity region. The leading contribution to the scattering amplitude in this kinematics has the form (in the Feynman gauge) [12]

$$A_{2 \rightarrow n+2} = g^2 \Gamma_a^{i_1} \frac{1}{q_1^2} p_a^{\mu_1} M_{\mu_1 \mu_2}^{i_1 i_2} p_b^{\mu_2} \frac{1}{q_2^2} \Gamma_b^{i_2}, \quad (\text{A.1})$$

where Γ is a (helicity conserving) vertex and i stands for the adjoint representation index. The incident particles have initial momenta p_a and p_b and the final ones $p'_a = p_a - q_1$ and $p'_b = p_b - q_2$:

$$p'_a = (1 - x_1)p_a - q_{1\perp} - \frac{2q_{1\perp}^2}{(1 - x_1)S} p_b, \quad p'_b = (1 - x_2)p_b - q_{2\perp} - \frac{2q_{2\perp}^2}{(1 - x_2)S} p_a,$$

where $p_a p_b = S/2$. In QMRK approximation one neglects the terms proportional to p_b in p'_a and proportional to p_a in p'_b . Now

$$q_1 = x_1 p_a + q_{1\perp}, \quad q_2 = x_2 p_b + q_{2\perp}$$

and $q_1^2 = q_{1\perp}^2$ and $q_2^2 = q_{2\perp}^2$

The explicit expression for Γ depends on the nature of incident particles. For example, if the incident particle a is a gluon the vertex has a form

$$\Gamma_a^i = 2f_{aa'}^i g_{\alpha\alpha'} \epsilon^\alpha(p_a) \epsilon^{\alpha'}(p'_a),$$

where $f_{aa'}^i$ is gauge algebra structure constant and ϵ is the gluon polarization vector. For quark scattering

$$\Gamma_a^i = 2t_{AA'}^i \bar{u}(p_a) \frac{\not{p}_b}{S} v(p'_a),$$

where $t_{AA'}^i$ is now a matrix in fundamental representation.

In general, color structure of (A.1) can be presented as $T_a^{i_1} T_{\dots}^{i_1 i_2} T_b^{i_2}$ where different T 's are color algebra generators in appropriate representation (\dots denote color indices of particles produced in the central rapidity region). The corresponding factor in the cross section reads

$$\text{tr}(T_a^{i_1} T_a^{i_1'}) \text{tr}(T_{\dots}^{i_1 i_2} T_{\dots}^{i_1' i_2'}) \text{tr}(T_b^{i_2} T_b^{i_2'})$$

Using the well known property of irreducible representations, $\text{tr}(T_a^{i_1} T_a^{i_1'}) \sim \delta^{i_1 i_1'}$, the summation over final and averaging over initial color indices can be converted into the averaging over i_1 and i_2 indices in $M_{\mu_1 \mu_2}^{i_1 i_2}$ in (A.1) with appropriate factors included into Γ 's (and thus into structure function definition). As these additional factors are completely independent of the structure of M we are having unambiguous determination of the factorization of the cross section into structure functions and a generalized cross section for the scattering of virtual particles described by them. The correct normalization is, in particular, crucial for getting a correct limit of collinear factorization in which the hard

cross section for the scattering of on-shell particles described by the usual ("integrated") structure functions should have correct color factors built in.

When particles produced include gluons the amplitude $M_{\mu_1\mu_2}$ gets contributions not only from diagrams of $2 \rightarrow n + 2$ type with n lines attached to the t -channel gluon, but also from diagrams with bremsstrahlung from p_a (p'_a) and p_b (p'_b) lines. These can be written in a form of (A.1) but, having no gluon with momentum q_1 (q_2) in the t -channel, give contribution to M proportional to $q_{1\perp}^2$ ($q_{2\perp}^2$). Thus the amplitude $M_{\mu_1\mu_2}$ has the form

$$M_{\mu_1\mu_2} = M_{\mu_1\mu_2}^{(1)} + \frac{q_1^2}{x_1 x_2 S} M_{\mu_1\mu_2}^{(2)} + \frac{q_2^2}{x_1 x_2 S} M_{\mu_1\mu_2}^{(3)} + \frac{q_1^2 q_2^2}{(x_1 x_2 S)^2} M_{\mu_1\mu_2}^{(4)},$$

Note that if even one of n particles is a gluon produced by bremsstrahlung from p_a (or p'_a) the corresponding diagram contributes to $M^{(2)}$. In the collinear factorization limit only $M^{(1)}$ contribution survives.

Our next goal is to show that the amplitude M can be rewritten in such a way, that the nonsense polarizations dominating the fluxes coming to the hard vertex can effectively be traded for the transverse ones providing a basis for interpreting the hard block contribution as a (modified) cross section. To do this let us consider the amplitude $A_{2 \rightarrow n+2}$ in the axial gauge with the gauge vector lying in (p_a, p_b) plane, $n = ap_a + bp_b$. In this gauge Γ 's do not change and the numerator of the gluon propagator is

$$d_{\mu\nu}(q) = g_{\mu\nu} - \frac{n_\mu q_\nu + q_\mu n_\nu}{n \cdot q} + n^2 \frac{q_\mu q_\nu}{(n \cdot q)^2}.$$

It is straightforward to check that the following important relations hold

$$p_a^\mu d_{\mu\nu}(q_1) = -\frac{1}{x_1} q_{1\perp,\nu}, \quad p_b^\mu d_{\mu\nu}(q_2) = -\frac{1}{x_2} q_{2\perp,\nu}. \quad (\text{A.2})$$

Let us now inspect how the structure of $p_a^{\mu_1} M_{\mu_1\mu_2} p_b^{\mu_2}$ changes in this gauge

$$\begin{aligned} p_a^{\mu_1} M_{\mu_1\mu_2}^{(1)} p_b^{\mu_2} &\rightarrow p_a^{\mu_1} d_{\mu_1}^{\nu_1}(q_1) M_{\nu_1\nu_2}^{(1)} d_{\mu_2}^{\nu_2}(q_1) p_b^{\mu_2}, \\ p_a^{\mu_1} M_{\mu_1\mu_2}^{(2)} p_b^{\mu_2} &\rightarrow p_a^{\mu_1} M_{\mu_1\nu_2}^{(2)} d_{\mu_2}^{\nu_2}(q_1) p_b^{\mu_2} \\ p_a^{\mu_1} M_{\mu_1\mu_2}^{(3)} p_b^{\mu_2} &\rightarrow p_a^{\mu_1} d_{\mu_1}^{\nu_1}(q_1) M_{\nu_1\nu_2}^{(3)} p_b^{\mu_2}, \\ p_a^{\mu_1} M_{\mu_1\mu_2}^{(4)} p_b^{\mu_2} &\rightarrow p_a^{\mu_1} M_{\mu_1\nu_2}^{(4)} p_b^{\mu_2}, \end{aligned} \quad (\text{A.3})$$

where $M^{(i)}$ have to be calculated in the new gauge. Now one can present $M^{(2)}$, $M^{(3)}$ and $M^{(4)}$ as follows

$$\begin{aligned} \tilde{M}_{\mu_1\mu_2}^{(2)} &= -\frac{q_{1\perp,\mu_1}}{x_2} \frac{p_a^{\nu_1}}{S} M_{\nu_1\nu_2}^{(2)} \\ \tilde{M}_{\mu_1\mu_2}^{(3)} &= -\frac{q_{2\perp,\mu_2}}{x_1} M_{\mu_1\nu_2}^{(3)} \frac{p_b^{\nu_2}}{S} \\ \tilde{M}_{\mu_1\mu_2}^{(4)} &= -\frac{q_{1\perp,\mu_1}}{x_2} \frac{q_{2\perp,\mu_2}}{x_1} \frac{p_a^{\nu_1}}{S} M_{\nu_1\nu_2}^{(4)} \frac{p_b^{\nu_2}}{S} \end{aligned}$$

Using now (A.2) we obtain

$$p_a^{\mu_1} M_{\mu_1\mu_2} p_b^{\mu_2} \rightarrow \frac{q_{1\perp}^{\mu_1}}{x_1} \tilde{M}_{\mu_1\mu_2} \frac{q_{2\perp}^{\mu_2}}{x_2},$$

where

$$\tilde{M} = M^{(1)} + \tilde{M}^{(2)} + \tilde{M}^{(3)} + \tilde{M}^{(4)}.$$

The amplitude $A_{2 \rightarrow n+2}$ projected onto the physical states of incoming and outgoing particles is, of course, gauge invariant. While gauge transformations do not change $\Gamma_{a,b}$ (when transforming from the covariant to the axial gauge) the $p_a^{\mu_1} M_{\mu_1\mu_2} p_b^{\mu_2}$ projected onto the physical polarizations of outgoing particles also remains the same (see (A.3)). This proves one can rewrite $M_{\mu_1\mu_2}$ in the form where the t-channel gluons having momenta $q_{1\perp}$ and $q_{2\perp}$ are having transverse polarizations in the original covariant gauge when the amplitude is projected onto the physical subspace.

Appendix B Cross sections of pair production in high energy factorization

Let us introduce the following notations

$$\begin{aligned} s &= 2(k_1 k_2 \text{ch}(\Delta y) - k_{1\perp} k_{2\perp}); \\ t &= -(q_{1\perp} - k_{1\perp})^2 - k_1 k_2 e^{\Delta y}, \quad u = -(q_{1\perp} - k_{2\perp})^2 - k_1 k_2 e^{-\Delta y}; \\ \Sigma &= x_1 x_2 S = k_1^2 + k_2^2 + 2k_1 k_2 \text{ch}(\Delta y), \end{aligned}$$

where $k_1 = \sqrt{k_{1\perp}^2}$, $k_2 = \sqrt{k_{2\perp}^2}$ and $k_{1\perp} k_{2\perp}$ is a dot product with 2d Euclidean metric.

The combined contribution from gluons and quarks (fermions) to gg scattering has the form (see (11))

$$\mathcal{A} = \mathcal{A}_{gluons} + \frac{n_f}{4N_c^3} \mathcal{A}_{fermions} \quad (\text{B.1})$$

B.1 $gg \rightarrow gg$

$$\mathcal{A}_{gluons} = \mathcal{A}_1 + \mathcal{A}_2$$

$$\begin{aligned} \mathcal{A}_1 = q_1^2 q_2^2 & \left\{ -\frac{1}{tu} + \frac{1}{4tu} \frac{q_1^2 q_2^2}{k_1^2 k_2^2} - \frac{e^{\Delta y}}{4tk_1 k_2} - \frac{e^{-\Delta y}}{4uk_1 k_2} + \frac{1}{4k_1^2 k_2^2} + \right. \\ & \frac{1}{\Sigma} \left[-\frac{2}{s} \left(1 + k_1 k_2 \left(\frac{1}{t} - \frac{1}{u} \right) \text{sh}(\Delta y) \right) + \frac{1}{2k_1 k_2} \left(1 + \frac{\Sigma}{s} \right) \text{ch}(\Delta y) - \right. \\ & \left. - \frac{q_1^2}{4s} \left[\left(1 + \frac{k_2}{k_1} e^{-\Delta y} \right) \frac{1}{t} + \left(1 + \frac{k_1}{k_2} e^{\Delta y} \right) \frac{1}{u} \right] \right. \\ & \left. \left. - \frac{q_2^2}{4s} \left[\left(1 + \frac{k_1}{k_2} e^{-\Delta y} \right) \frac{1}{t} + \left(1 + \frac{k_2}{k_1} e^{\Delta y} \right) \frac{1}{u} \right] \right] \right\} \quad (\text{B.2}) \end{aligned}$$

$$\mathcal{A}_2 = \frac{1}{2} \left\{ \left(\frac{(k_{1\perp} - q_{1\perp})^2 (k_{2\perp} - q_{1\perp})^2 - k_1^2 k_2^2}{tu} \right)^2 - \frac{1}{4} \left(\frac{(k_{2\perp} - q_{1\perp})^2 - k_1 k_2 e^{-\Delta y}}{(k_{2\perp} - q_{1\perp})^2 + k_1 k_2 e^{-\Delta y}} - \frac{E}{s} \right) \left(\frac{(k_{1\perp} - q_{1\perp})^2 - k_1 k_2 e^{\Delta y}}{(k_{1\perp} - q_{1\perp})^2 + k_1 k_2 e^{\Delta y}} + \frac{E}{s} \right) \right\},$$

$$E = (q_{1\perp} - q_{2\perp})(k_{1\perp} - k_{2\perp}) - \frac{1}{\Sigma} (q_1^2 - q_2^2)(k_1^2 - k_2^2) + 2k_1 k_2 \text{sh}(\Delta y) \left(1 - \frac{q_1^2 + q_2^2}{\Sigma} \right).$$

B.2 $gg \rightarrow q\bar{q}$

$$\mathcal{A}_{fermions} = N_c^2 \mathcal{A}_{1f} + \mathcal{A}_{2f}$$

$$\mathcal{A}_{1f} = \left\{ 2 \frac{q_1^2 q_2^2}{s\Sigma} \left(1 + k_1 k_2 \text{sh}(\Delta y) \left(\frac{1}{t} - \frac{1}{u} \right) \right) - \left(\frac{(k_{1\perp} - q_{1\perp})^2 (k_{2\perp} - q_{1\perp})^2 - k_1^2 k_2^2}{tu} \right)^2 + \frac{1}{2} \left(\frac{(k_{2\perp} - q_{1\perp})^2 - k_1 k_2 e^{-\Delta y}}{(k_{2\perp} - q_{1\perp})^2 + k_1 k_2 e^{-\Delta y}} - \frac{E}{s} \right) \left(\frac{(k_{1\perp} - q_{1\perp})^2 - k_1 k_2 e^{\Delta y}}{(k_{1\perp} - q_{1\perp})^2 + k_1 k_2 e^{\Delta y}} + \frac{E}{s} \right) \right\} \quad (\text{B.3})$$

and

$$\mathcal{A}_{2f} = \left\{ \left(\frac{(k_{1\perp} - q_{1\perp})^2 (k_{2\perp} - q_{1\perp})^2 - k_1^2 k_2^2}{tu} \right)^2 - \frac{q_1^2 q_2^2}{tu} \right\}$$

where E is the same as for gluons.

In multy-Regge kinematics only term leading in $\Delta y \rightarrow \infty$ survives and

$$\mathcal{A}_{MRK} = \mathcal{A}_{MRK,gluons} = \frac{q_1^2 q_2^2}{k_1^2 k_2^2}$$

References

- [1] G. Marchesini *Nucl. Phys.* **B445** (1995) 40;
J.R. Forshaw, A. Sabio Vera *Phys. Lett.* **B440** (1998) 141;
- [2] G.P. Salam, "Soft Emissions and the Equivalence of BFKL and CCFM Final States",
[hep-ph/9902324]
- [3] E. Bonvin *et al.* (WA70 Coll.) *Phys. Lett.* **B236** (1990) 523;
F. Abe *et al.* (CDF Coll.) *Phys. Rev. Lett.* **70** (1993) 2232
- [4] L. Apanasevich *et al.* (E706 Fermilab Coll.) *Phys. Rev. Lett.* **81** (1998) 2642
- [5] J.C. Collins, D.E. Soper, G. Sterman *in* Perturbative quantum chromodynamics,
ed. A.H.Mueller (World Scientific, Singapore, 1989) and references therein

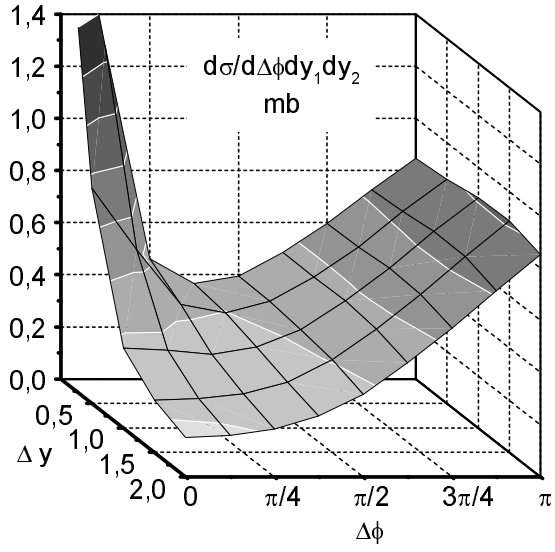
- [6] V.N. Gribov and L.N. Lipatov *Sov. Journ. Nucl. Phys.* **15** (1972) 438;
G. Altarelli and G. Parisi *Nucl. Phys.* **B126** (1977) 298;
Yu. L. Dokshitzer *Sov. Phys. JETP* **46** (1977) 641
- [7] L.N. Lipatov *Sov. J. Nucl. Phys.* **23** (1976) 338;
E.A.Kuraev, L.N. Lipatov, V.S. Fadin *Sov. Phys.JETP* **45** (1977) 199;
Ya. Balitskii, L.N. Lipatov *Sov. J. Nucl. Phys.* **28** (1978) 6
- [8] S. Catani, F. Fioranti, G. Marchesini *Nucl. Phys.* **B336** (1990) 18
- [9] S. Catani, M. Ciafoloni, F. Hautmann *Nucl. Phys.* **B366** (1991) 135
- [10] E.M. Levin, M.G. Ryskin *Yad. Fiz.* **32** (1980) 802 (in Russian)
- [11] V.S. Fadin, N.L. Lipatov *Sov. J. Yad. Phys.* **50** (1989) 1141
- [12] V.S. Fadin, N.L. Lipatov *Nucl. Phys.* **B477** (1996) 767
- [13] J.F. Gunion, G. Berch *Phys. Rev. D* **25** (1982) 746
- [14] K.J. Eskola, A.V. Leonidov, P.V. Ruuskanen *Nucl. Phys.* **B481** (1996) 704
- [15] V.S. Fadin, M.I. Kotsky, L.N. Lipatov *Gluon pair production in the quasi-multi-Regge kinematics* (1997) [hep-ph/9704267]
- [16] V.S. Fadin, R. Fiore, A. Flachi, M.I. Kotsky *Phys. Lett.* **B422** (1998) 287
- [17] V. Del Duca, C.R. Schmidt *Phys. Rev. D* **49** (1994) 177, 4510; *Phys. Rev. D* **51** (1995) 2150; *Nucl. Phys. Proc. Suppl.* **39BC** (1995) 137; [hep-ph/9410341];
W.J. Stirling *Nucl. Phys.* **B423** (1994) 56
- [18] V.S.Fadin, L.N.Lipatov *Phys.Lett.* **B429** (1998) 127;
S.J. Brodsky, V.S. Fadin, V.T. Kim, L.N. Lipatov, G.B. Pivovarov, "The QCD Pomeron with Optimal Renormalization" [hep-ph/9901229]
- [19] L. McLerran, R. Venugopalan *Phys.Rev.* **D49** (1994) 2233, 3352;
J. Jalilian-Marian, A. Kovner, L. McLerran, H. Weigert *Phys.Rev.* **D55** (1997) 5414;
J. Jalilian-Marian, A. Kovner, A. Leonidov, L. McLerran, H. Weigert *Nucl.Phys.* **B504** (1997) 415;
J. Jalilian-Marian, A. Kovner, H. Weigert *Phys.Rev.* **D59** (1999) ,[hep-ph/9709432]
- [20] L. Gribov, E. Levin, and M. Ryskin *Phys.Rept* **100** (1983) 1-150
- [21] H.-L. Lai et al *Eur.Phys.J.* **C12** (2000) 375
- [22] A.J. Askew, J. Kwiecinski, A.D. Martin, P.J. Sutton *Phys. Rev.* **D49** (1994) 4402
- [23] M.A. Kimber, A.D. Martin, M.G. Ryskin Unintegrated parton distributions and prompt photon hadronization hep-ph/9911379

- [24] G. Marchesini, B. Webber *Nuc. Phys.* **B310** (1988) 461
- [25] Yu.L. Dokshitzer, D.I. Dyakonov, S.I.Troyan *Phys. Rep.* **58** (1980) 269
- [26] N.M. Korobov "Teoretikochislovye metody v priblizhennom analize" ("Number theory methods in approximate analysis", in Russian). Moscow, Fizmatgiz, 1963.

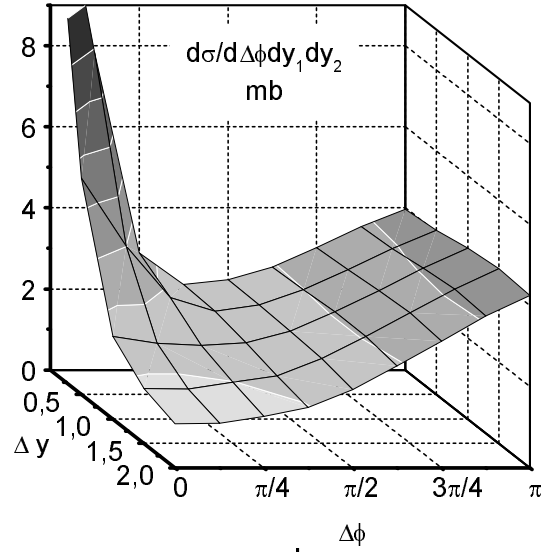
Figure captions

The cross sections depicted in figures are calculated for unintegrated structure functions CTEQ5M [21] and AKMS [22] with constant $\alpha_s = 0.2$. Gluon and quark contributions (with $n_f = 5$) are added up.

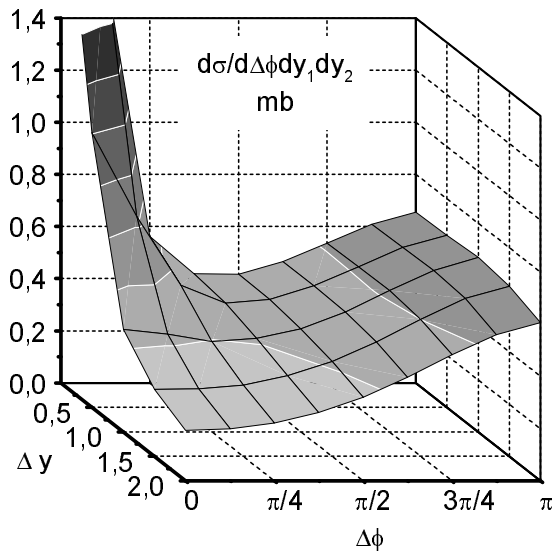
- Fig. 1** Cross section Eq. (12) calculated for $k_0 = 2 \text{ GeV}$, $y_0 = 0$ and $\Delta y \in [0, 2]$
a with CTEQ5M structure functions, $\sqrt{S} = 1.8 \text{ TeV}$
b with CTEQ5M structure functions, $\sqrt{S} = 14 \text{ TeV}$
c with AKMS structure functions, $\sqrt{S} = 1.8 \text{ TeV}$
d with AKMS structure functions, $\sqrt{S} = 14 \text{ TeV}$
- Fig. 2** Angular asymmetry $\rho(\Delta\phi)$ for $k_0 = 2 \text{ GeV}$, $y_0 = 0$ and $\Delta y = 0.5, 1, 2$. Specific parameters for **a, b, c, d** same as above.
- Fig. 3** Angular asymmetry $\rho(\Delta\phi)$ for $y_{1,2} = \pm 0.5$ and $k_0 = 4, 8, 12, 16 \text{ GeV}$. Specific parameters for **a, b, c, d** are the same as earlier.
- Fig. 4** Momentum asymmetry Eq. (15) for $y_{1,2} = \pm 0.5$. Specific parameters for **a, b, c, d** same as above.



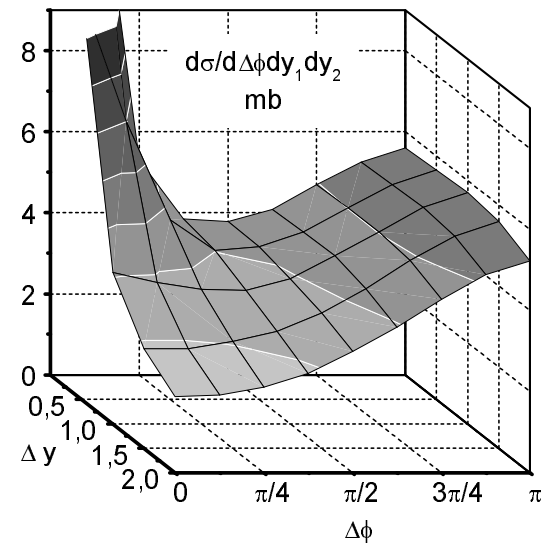
a



b



c



d

Figure 1

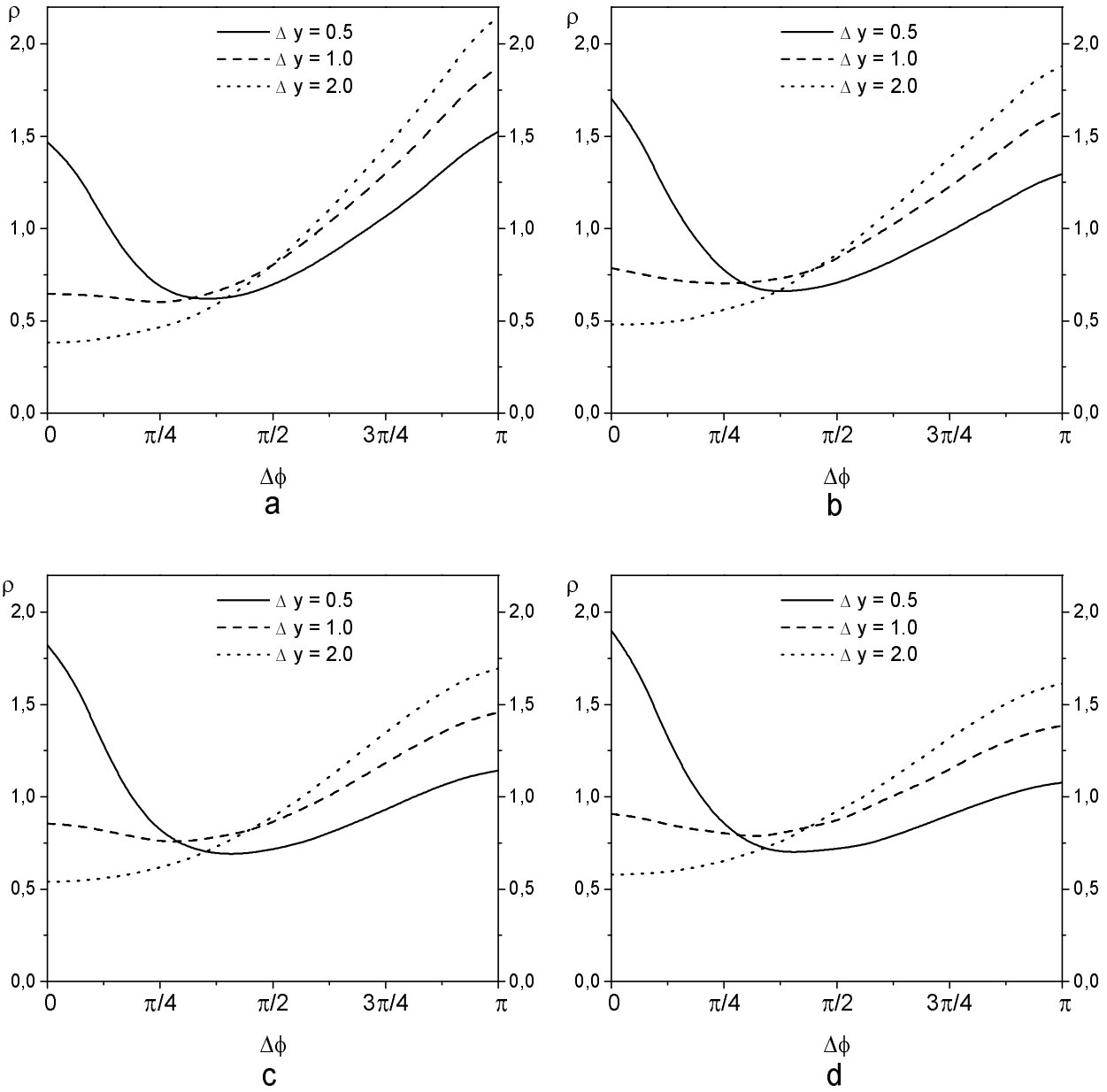


Figure 2

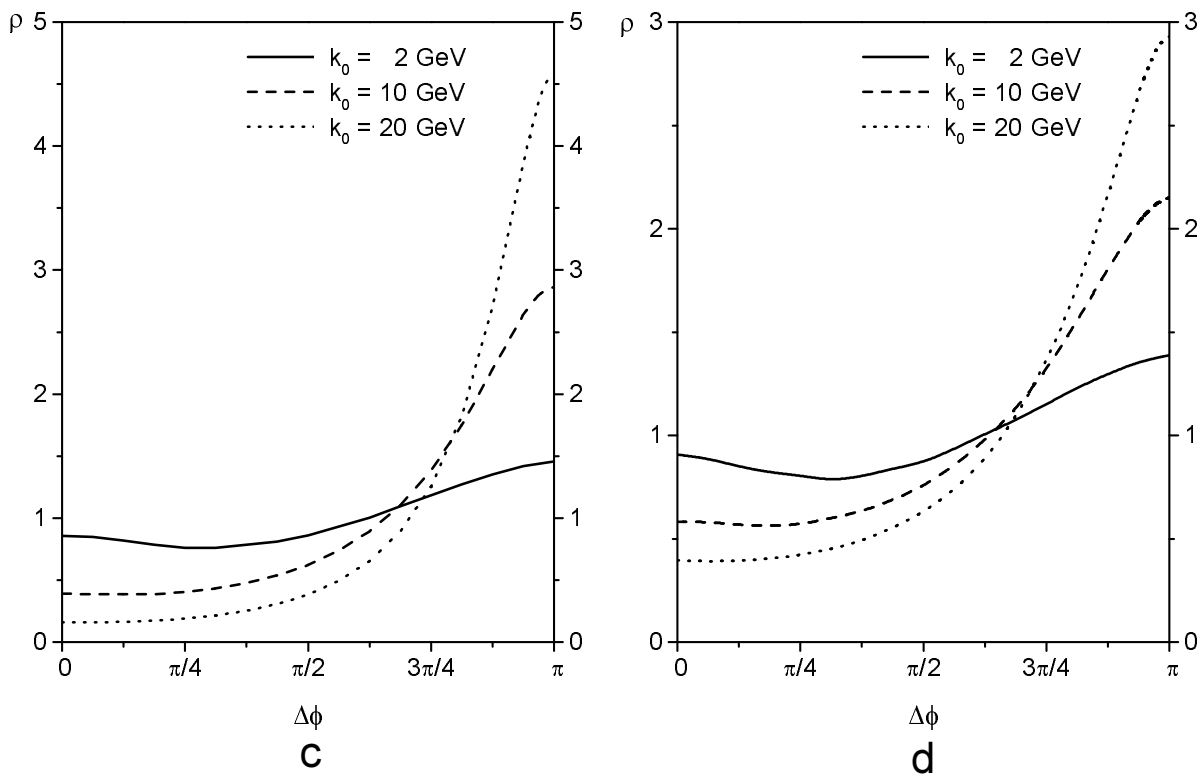
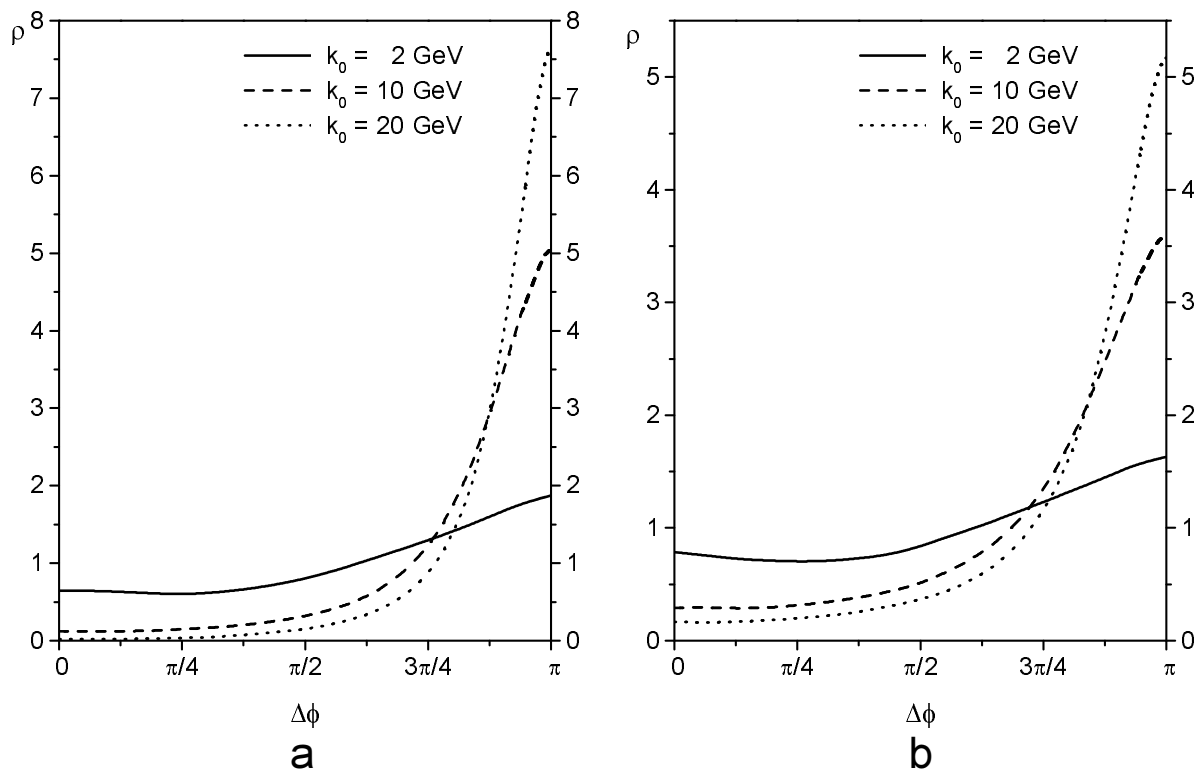
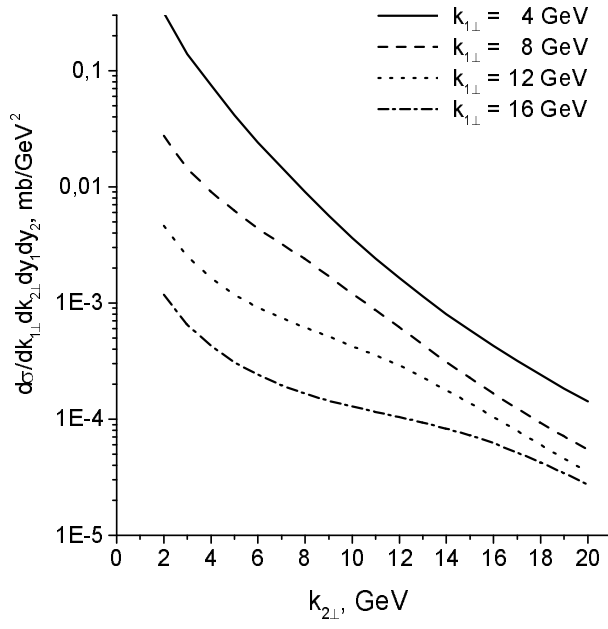
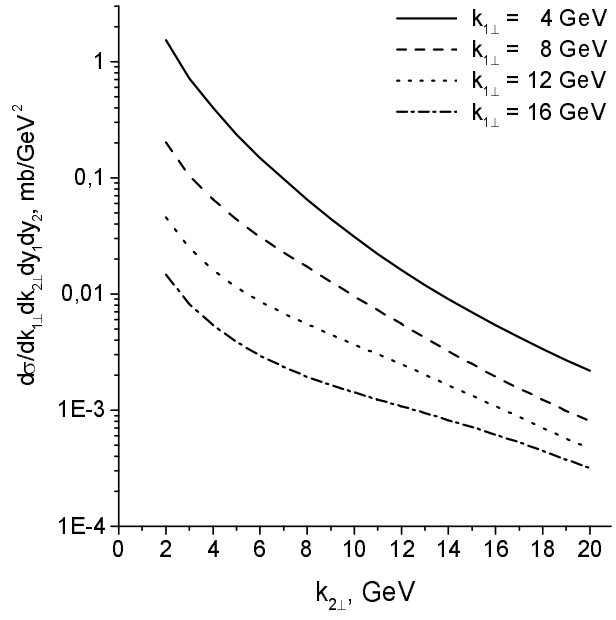


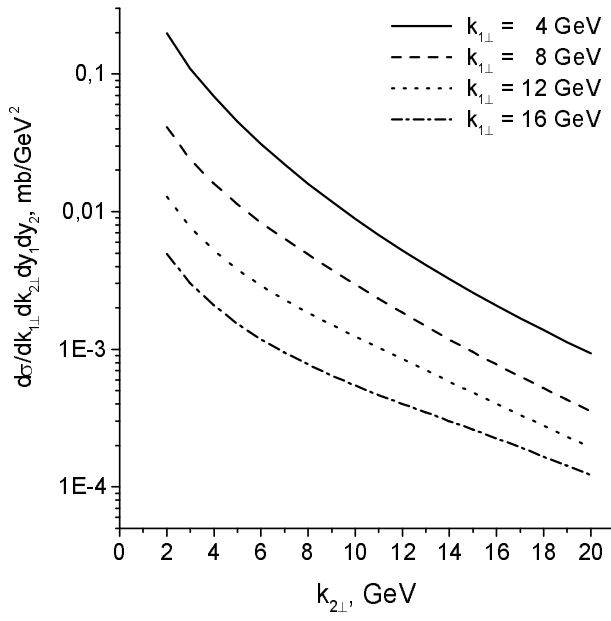
Figure 3



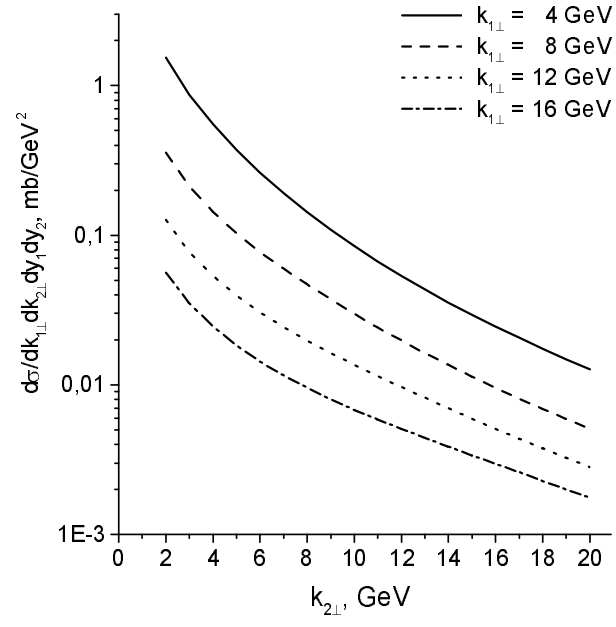
a



b



c



d

Figure 4